Rigid-rod derived amorphous polydiacetylenes

Michael A. Schen*‡, Kristine Kotowski* and James Cline†
*National Institute of Standards and Technology, *Polymers Division and †Ceramics Division, Gaithersburg, MD 20899, USA*
(Received 10 August 1990; accepted 24 October 1990)

During our investigations of diacetylene monomers that exhibit thermotropic liquid-crystal phase behaviour, it was discovered that spontaneous and rapid thermal polymerization of the isotropic monomer melt takes place with some of the compounds examined. In the diacetylene monomer series containing symmetrically disubstituted 4-oxybenzylidene-4'-n-octylaniline (OBOA) side-groups attached to a butadiyne core via a polymethylene spacer, monomer liquid crystallinity is seen in the lower members of the series yet facile polymerization in the isotropic monomer melt is observed only in the lowest member of the series. This compound, 1OBOA, is believed to be rod-like in structure. It is this microstructural architecture that is believed to be responsible for imparting this unique combination of polymerization and polymer properties. Traditional molecularly flexible diacetylene monomers and the more flexible homologues in the *n*OBOA series do not show such facile melt-phase reactivity and do not allow the synthesis of purely amorphous conjugated polymer films.

(Keywords: polydiacetylenes; liquid-crystal monomers; rigid rods; amorphous polymers; X-ray scattering; morphology; ultraviolet, visible, near-infra-red spectroscopy)

INTRODUCTION

Polydiacetylenes (PDAs) have long been viewed to be unique because of the facile manner in which monomer to polymer conversion takes place in the condensed crystal phase. This 'topochemical' polymerization process, as first explored by Wegner and coworkers[1], typically involves either the thermal, ultra-violet, or gamma-radiation initiation of monomer in the crystal phase and yields highly ordered molecular assemblies of electroactive polymer. Such highly oriented samples have shown very large non-resonant third-order non-linear optical susceptibilities[2] and low optical losses for shear-crystallized polymers[3].

The extent to which defect-free *monomer* crystals can be obtained appears to be strongly related to the method of monomer crystallization. Thakur and coworkers[3] report that shear-crystallized toluene sulphonate (TS) monomer has fewer defects such as voids, cracks, grain boundaries, etc., than solution-crystallized monomer. The extent to which *polymer* crystals free of crystallographic defects can be obtained depends on the specific monomer and method of initiation. TS monomer, crystallized by the method of Thakur[3] and thermally polymerized, gives single crystals free of scattering defects. Poly[1,6-bis-(*N*-carbazolyl)-2,4-hexadiyne] (DCHD), on the other hand, may or may not be free of scattering centres depending on whether it was prepared thermally or by gamma irradiation[4]. Gamma-polymerized poly (-DCHD) shows no signs of polymerization-induced crystal disintegration, whereas crystals polymerized thermally reveal extensive crystal surface defects. In an all-optical application, polymer films that are either highly organized and single-crystalline or that are completely amorphous exhibit sufficiently low optical losses to be device-practical. Nearly all work on PDA has focused on either single-crystalline or solution-regenerated, semicrystalline films.

To understand better how monomer crystal structure impacts monomer polymerizability, Bloor and coworkers[5] have studied a number of reactive and non-reactive diacetylene monomer systems in the context of earlier models by Schmidt[6] and Baughman[7]. In these models, 1,4-polymerization is allowed under conditions in which residue rotation or rotation in conjunction with translation bring the reactive carbon centres of adjacent molecules within 0.4 nm of each other in the monomer lattice. Combining crystallographic and polymerization reactivity data, it was discovered that, in a plot of centre of gravity separation distance d between adjacent monomer molecules and molecular tilt angle ϕ within the stack, there exists an envelope of reactivity whereby solid-state polymerization is observed. Beyond the envelope, when separation distances exceed 0.4 nm, facile solid-state polymerization is not seen.

Such strict criteria for observing polymerizability in the condensed phase are questioned, however, because of polymerization which occurs in other than completely ordered systems. There now exist many polymer systems which contain diacetylene linkages within the repeat unit of a polymer backbone. Rubner and coworkers have prepared and studied such systems, including segmented polyurethane–diacetylene[8] and polyamide–diacetylene[9] copolymers. In the former study, the diacetylene group was incorporated within the urethane hard segment. From differential scanning calorimetry (d.s.c.), it is seen that spontaneous cross-polymerization of diacetylene

Paper presented at Speciality Polymers '90, 8–10 August 1990, The Johns Hopkins University, Baltimore, MD, USA
‡ To whom correspondence should be addressed

0032-3861/91/101843-08

units within the polymer chains occurs upon heating. Polymerization does not take place within the hard-segment crystalline domains. Instead, polymerization is seen to begin after melting of the hard segments; that is to say, once the polymer becomes disordered. In the polyamide–diacetylene system, similar behaviour is observed, with d.s.c. data indicating spontaneous polymerization after melting of polymer crystallites. Because of the high temperatures at which polymerization is occurring (from 200 to 300°C), it is suggested that simultaneous polymerization–degradation is actually occurring. In an analogous system studied by Pail *et al.*, segmented polyester–diacetylene polymer also shows the same spontaneous polymerization behaviour in the polymer melt[10].

Recently we have been studying the polymerization behaviour of low-molecular-mass liquid crystals (LCs) and their non-liquid-crystalline homologues containing the 1,4-disubstituted 1,3-butadiyne moiety[11]. Depending upon the degree to which vibrational and rotational relaxations of the substituents are decoupled from the diacetylene core, thermotropic liquid-crystalline polymorphism or simple crystal-to-isotropic melting is observed[12]. In the system that incorporates the symmetrically disubstituted 4-oxybenzylidene-4′-n-octylaniline mesogen (designated *n*OBOA, where *n* indicates the number of methylene carbon units bridging the diacetylene and mesogen units), reactivity towards thermal polymerization is observed in the $n=1$ monomer when the monomer enters the liquid-crystalline regime[12]. Spontaneous and complete polymerization in the isotropic monomer melt is also observed.

Depending on the regime within which polymerization is conducted, polymers from the 1OBOA monomer with completely different micromorphologies are obtained[13]. Polymerization in the low-temperature, highly ordered smectic region results in polymer that is interpreted from X-ray scattering to possess a two-dimensionally disordered, layer-like microstructure. Polymerization conducted within the isotropic melt gives highly coloured polymer glasses.

This paper reports on the polymerization behaviour of homologues of the *n*OBOA monomer series where $n=1$, 3 and 4, with special emphasis directed to the phenomenon of melt-phase polymerization of rod-like molecules. This important behavioural aspect of rod-like diacetylenes, both liquid-crystalline and non-liquid-crystalline, is in stark contrast to the relatively non-reactive nature of architecturally flexible diacetylenes in the disordered monomer melt. Polymer characterization indicates that a completely amorphous polymer glass is obtained which shows no thermal transitions before decomposition begins. It is believed that such new types of completely amorphous PDAs potentially offer a new means for obtaining temperature-stable, low-loss optical films.

EXPERIMENTAL

Monomers under discussion include the $n=1$, 3 and 4 homologues of symmetrically 1,4-disubstituted 1,3-butadiyne which incorporate as substituents the liquid-crystalline mesogen *n*OBOA. The molecular structure of *n*OBOA is shown below. The synthesis and thermal properties have been described elsewhere[11].

n-OBOA $n = 1, 3, 4$

$$R—C\equiv C-C\equiv C—R$$

$$R= -(CH_2)_n O-\langle\bigcirc\rangle-CH=N-\langle\bigcirc\rangle-(CH_2)_7-CH_3$$

Differential scanning calorimetry measurements were conducted at a scan rate of 10°C min^{-1} unless otherwise noted using a Perkin–Elmer DSC-II*. Optical measurements were conducted using a Perkin–Elmer Lambda 9 UV/Vis/NIR spectrophotometer with a Lab Sphere DRATA-9 integrating sphere attachment*. Diffuse transmission spectra were collected at room temperature using finely divided monomer sandwiched between quartz plates. Spectral data were normalized to 320 nm after first subtracting a constant absorption factor needed to establish a zero baseline between 1000 and 1100 nm. Difference spectra and intensity integration were obtained using normalized data. Fourier-transform infra-red (*FT*i.r.) data were collected at room temperature using KBr pellets that had been made using the original monomer. Pellets were then heated under vacuum to polymerize the monomer. Room-temperature X-ray scattering was performed with Cu K_α radiation on packed powders of monomer containing randomly dispersed NIST standard reference material (SRM) No. 675 (fluorophlagopite) for *d*-spacing calibration. Samples were heated either in vacuum or under a nitrogen blanket for prescribed times, then mounted within the diffractometer. The diffractometer was equipped with theta compensating slit and graphite beam diffracted monochromator. Integrated peak intensities were normalized to $2\theta=8.86°$ reflection of the SRM.

RESULTS AND DISCUSSION

In the *n*OBOA series, a number of temperature–microphase profiles are observed depending on the spacer length used to bridge the diacetylene core to the mesogenic side-groups. *Figure 1* shows the d.s.c. scans for the $n=1$, 3 and 4 monomers along with that for poly(1OBOA). In all three monomers multiple phase transitions are observed. In the case of 4OBOA, the endotherm at 94°C is seen by optical microscopy to be a crystal–crystal transition and the one at 127°C is a crystal–isotropic melting. A second scan to higher temperatures shows no additional transitions. Crystal–liquid crystal transitions preceded by multiple crystal–crystal transitions have also been seen in 4,4′-dialkanoyloxydiphenyldiacetylene diester liquid crystals reported by Blumstein and coworkers[14]. In general, diacetylene monomers generally exhibit multiple crystal structures depending on crystallization conditions. Heating 3OBOA reveals two endothermic transitions with maxima at 169 and 178°C. Dark-field optical microscopy reveals the first to be a crystal–liquid crystal

*Material suppliers, commercial equipment, or instruments are identified in this paper to specify adequately the experimental procedure. Such identification does not imply recommendation or endorsement by the National Institute of Standards and Technology or the United States Government

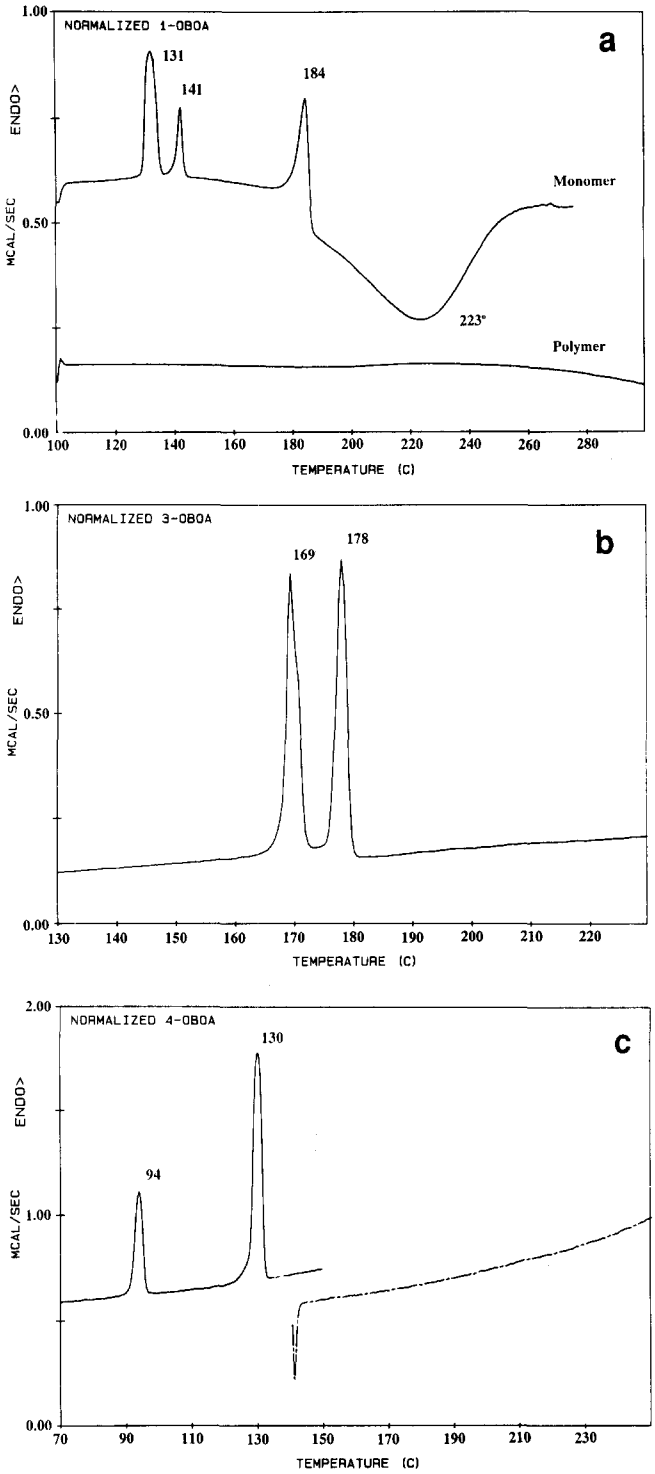

Figure 1 Normalized d.s.c. scans for: (a) 1OBOA monomer and amorphous polymer; (b) 3OBOA monomer; and (c) 4OBOA monomer

transition and the second a liquid crystal–isotropic melting[15]. Optical textures indicate either a nematic or disordered smectic LC structure between the two endotherms for 3OBOA. In the case of 1OBOA, three endothermic transitions are observed in the monomer. Previously, these have been assigned to the following transitions[13]:

$$\text{Crystal} \xrightarrow{130^\circ\text{C}} \text{Smectic G or H} \xrightarrow{140^\circ\text{C}} \text{Smectic C} \xrightarrow{183^\circ\text{C}} \text{Isotropic}$$

Only in the $n=1$ homologue is there evidence of spontaneous isotropic-phase polymerization, as shown by the large exotherm in *Figure 1a*. At a heating rate of 10°C min^{-1}, polymerization rate reaches a maximum at 223°C. *Figure 1a* also shows a scan for poly(1OBOA) polymerized at 171°C. No thermal transitions are observed, excluding an exothermic baseline drift above ~260°C. Previously reported thermal gravimetric analysis results for 1OBOA monomer show the onset of weight loss and material decomposition at 255°C[11].

Because of the proximity of the clearing point, i.e. the temperature at which the material goes isotropic, to the polymerization exotherm, determination of the heat of reaction is rendered somewhat difficult from d.s.c. data. An average from three separate experiments gives an estimation for ΔH_p of 247 ± 21 kJ mol^{-1}. Alternatively, isothermal calorimetry experiments conducted at 190°C for 2 h give a ΔH_p of 273 kJ mol^{-1}. These numbers are larger than the ≈ 150 kJ mol^{-1} polymerization enthalpies associated with the crystal-phase polymerization of diacetylene monomers[15], but are comparable to the enthalpy of reaction (≈ 240 kJ mol^{-1}) reported by Milburn and coworkers[16,17] for rod-like 4,4′-disubstituted diphenyldiacetylenes. Though some of Milburn's compounds do not exhibit liquid-crystal behaviour, spontaneous melt polymerization is reported. As of yet, no adequate explanation has been found to account for the differences in enthalpies between melt-phase and crystal-phase polymerizations.

It is useful to observe in *Figure 1* that, for the $n=3$ and 4 monomers, the baseline slope remains virtually unchanged as the temperature passes through the various first-order transitions. In other words, unlike the case for 1OBOA monomer, no sign of heat evolution is observed. Samples of 1OBOA and 3OBOA were held at 170°C, within the liquid-crystalline region for each material. With the $n=1$ homologue, complete polymer conversion occurs within 2 h as determined from isothermal calorimetry. In contrast, with the $n=3$ homologue, only a 17% decrease in monomer content due to polymerization is recorded after 4 h annealing at 170°C. This is based on measuring the monomer heat of fusion after annealing. Similar experiments with all three homologues held at 190°C – within the disordered monomer melt – show reduced polymerization reactivity as the spacer length increases within the

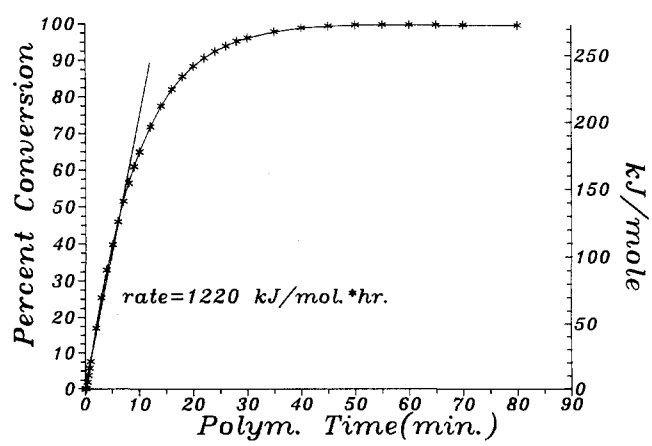

Figure 2 Conversion curve for the 190°C isotropic melt polymerization of 1OBOA based on isothermal calorimetry data

molecule. With the $n=1$ homologue, 99% monomer-to-polymer conversion is achieved after 40 min as determined from isothermal calorimetry experiments (*Figure 2*). In the case of 3OBOA, only a 42% decrease in monomer content and therefore extent of polymerization was recorded after 8 h of heating. With the $n=4$ homologue, only a 17% diminution in monomer content was recorded also after 8 h at 190°C. Because of the extremely slow reaction rates for the $n=3$ and 4 homologues and instrumental limitations, isothermal calorimetry experiments were never able to extend to sufficiently long times to observe a flattening out of the conversion curve. Therefore, it is unknown whether these two monomers would continue to react to complete conversion given much longer reaction times or if there exists a limitation to which conversion can occur.

Kinetic data for the 1OBOA thermal polymerization in conjunction with the 190°C, 8 h conversion data for the $n=3$ and 4 homologues indicate that, relative to the $n=1$ homologue, 3OBOA is roughly 90 times less reactive and 4OBOA is over 200 times less reactive. It is important to note in *Figure 2* that no induction period is observed. This is in contrast with the thermal polymerization of many other diacetylene monomers, most notably TS monomer[18]. Autocatalytic polymerization behaviour, as evidenced by an induction period followed by a regime of enhanced reactivity, is seen to reflect induced strain resulting from packing mismatch of the monomer-rich and polymer-rich phases[19]. The absence of an induction period in the 1OBOA conversion curve indicates the homogeneous nature of the polymerization. Little if any internal strain is expected given the reduced viscosity of the phase within which polymerization is occurring.

Figure 3 shows the evolution of the normalized u.v./vis./n.i.r. absorption spectra for the 190°C polymerization of the $n=1$ homologue. The spectral irregularities centred about 900 nm are an instrumental artifact due to detector switch-over. The nascent monomer has an absorption edge at ~400 nm (3.1 eV), which is due to excitation of the conjugated aromatic imine substituents. Assuming this contribution to remain constant during the course of polymerization, as was verified from *FT*i.r. results (see below), difference spectra can be generated, which show more clearly the optical changes arising from polymer formation. After 5 min, a strong absorption with a maximum at ~430 nm and shoulder at ~475 nm appears. After 15 min, the polymer absorption maximum remains at ~430 nm while the shoulder has shifted to higher wavelengths, ~510 nm. Over the entire reaction time, a continuous shift of the absorption edge to ever lower energies is observed. *Figure 4* shows the integrated absorption intensities derived from the normalized spectra for the 190 and 150°C polymerization of 1OBOA. Within the scatter limits of the data, the total intensities appear to saturate after 60 min at 190°C. It is interesting to note that in *Figure 3*, after 60 min, there is a decrease of intensity in the 'plateau' region below 550 nm while the edge is continuing to move to lower energies (~2.1 eV) even up to the 90 min point.

Figure 4 also shows the integrated absorption data for a 1OBOA polymerization conducted at 150°C and within the smectic C regime. As is seen, data from both temperatures do not show the presence of a polymerization induction period. Also, the total absorption intensity is greater for the 190°C reaction than for the 150°C polymerization. Though this observation requires further consideration, it may reflect a greater degree of conversion in the disordered melt in contrast to the ordered smectic phase. Alternatively, it may also signal formation of different colour centres, i.e. polymer backbone structure, within the two materials.

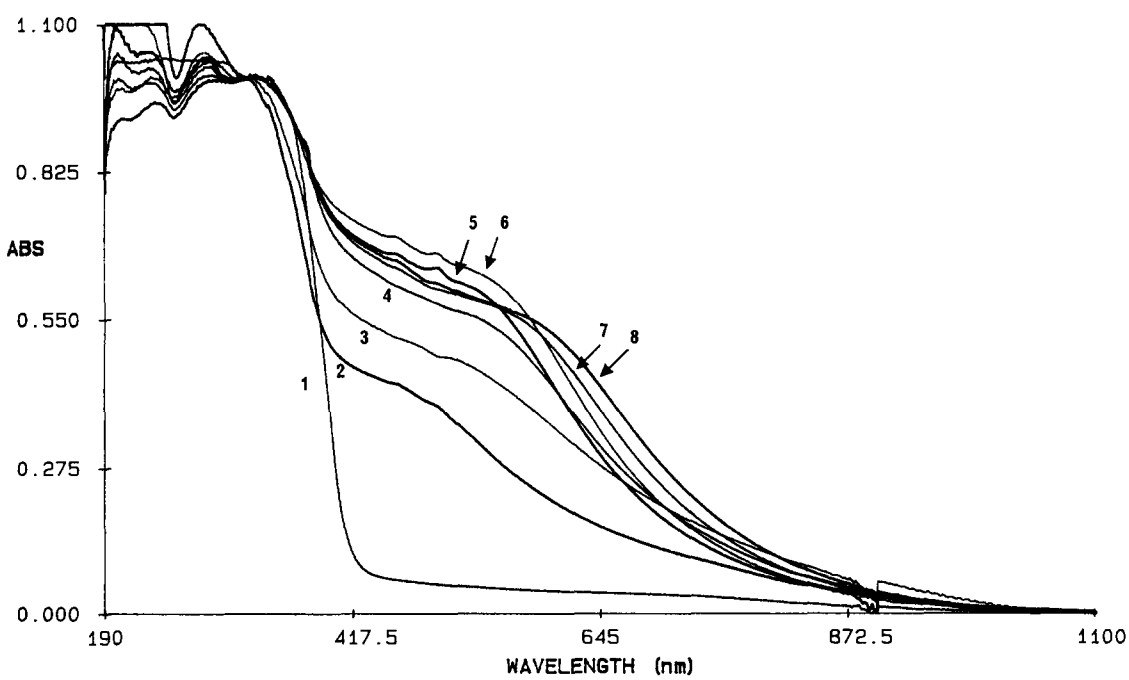

Figure 3 Normalized u.v./vis/n.i.r. absorption spectra for the 190°C 1OBOA polymerization: (1) monomer; (2) 5 min; (3) 15 min; (4) 30 min; (5) 40 min; (6) 60 min; (7) 75 min; and (8) 90 min polymerization time

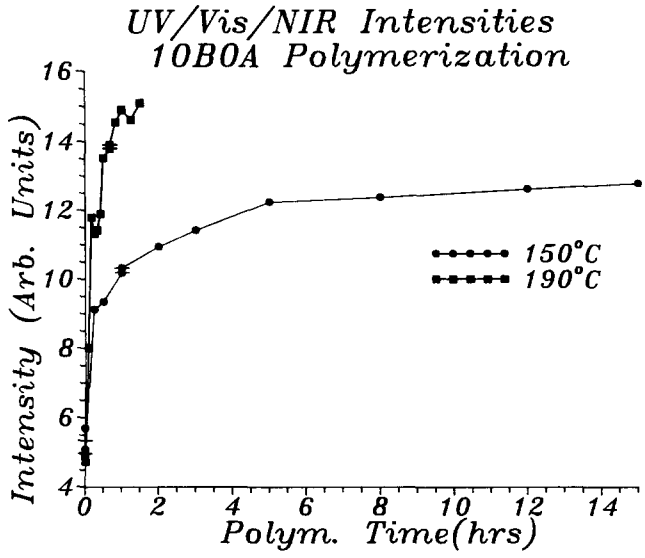

Figure 4 Evolution of normalized u.v./vis/n.i.r. integrated absorption intensities for the 150°C and 190°C polymerization of 1OBOA monomer

As previously mentioned, Rubner and coworkers[8,9] have observed that thermal annealing of diacetylene-containing segmented polyurethanes and polyamides also undergo spontaneous polymerization in the disordered polymer melt as evidenced by a large, high-temperature exotherm. Because of the high temperatures, ranging from 200 to 300°C, at which polymerization is taking place, the authors believe that simultaneous polymerization and degradation is taking place. During our investigations, we have been using *FT*i.r. to check if chemical degradation accompanies high-temperature polymerization. *Figure 5* shows the *FT*i.r. spectra within the 'fingerprint' region for 1OBOA monomer (curve A) and polymer after polymerization at 170°C for 90 min (curve B) and 190°C for 80 min (curve C). Peak assignments are listed in *Table 1*.

As is seen, spectra from both polymer samples show vibrational bands similar to those observed in the monomer. Because of the high density of aromatic imine side-groups in the polymer and the infra-red inactivity of the all-carbon polymer backbone, infra-red spectroscopy is particularly well suited for examining

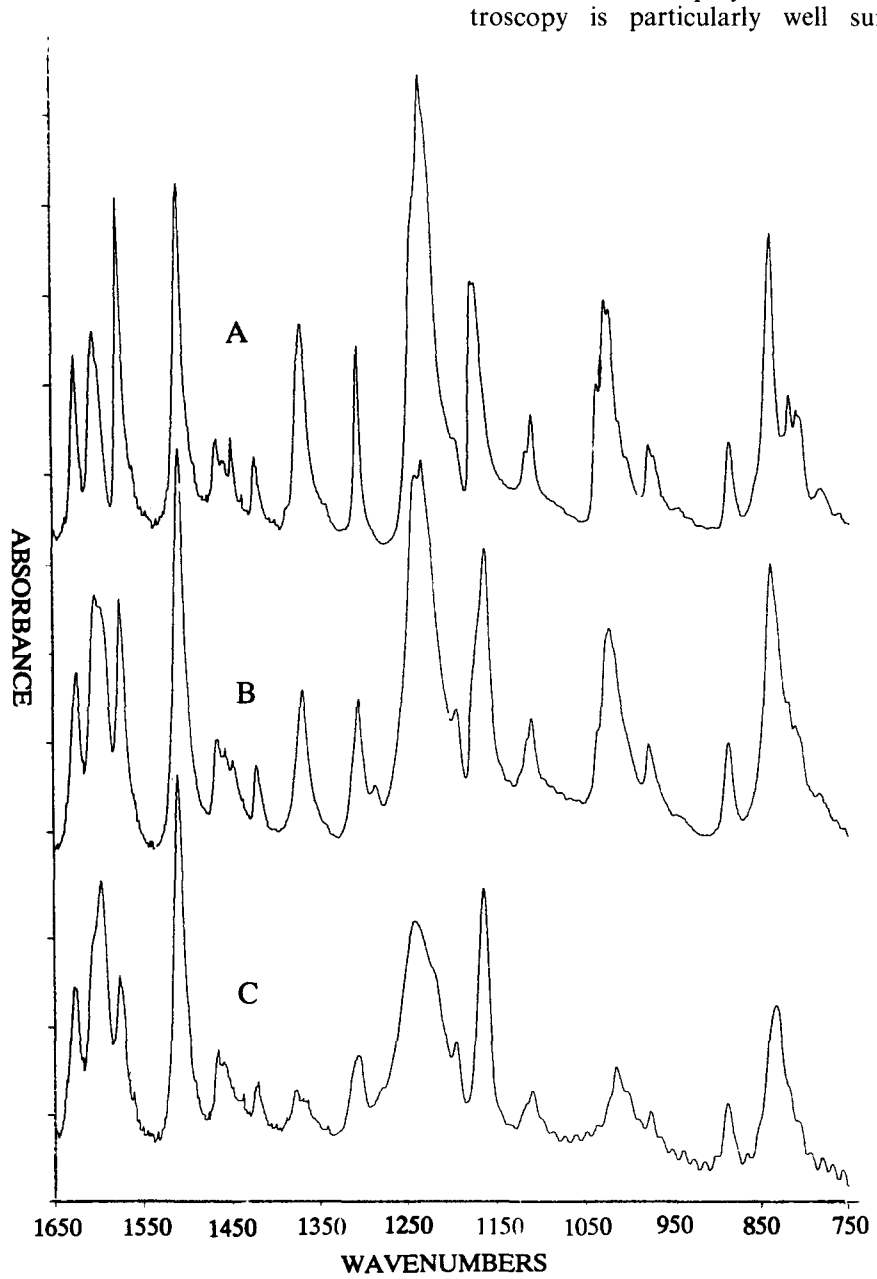

Figure 5 *FT*i.r. 'fingerprint' spectra of 1OBOA: (A) monomer; (B) polymer (170°C/90 min); and (C) polymer (190°C/80 min)

Table 1

Wavenumber (cm^{-1})	Assignment
1626	C=N stretch
1600; 1576	Ar C=C stretch
1508; 1421	Ar semicircle stretch
1465; 1448; 1437	CH_2 deformation
1377	CH_2 wag
1305	CH_2 twist
1233; 1240	Aromatic C—O stretch
1172; 1162; 1108	Ar ring stretch
1021; 1014	Aliphatic C—O stretch
977; 839; 807	Ar C—H bending
886	CH_2, CH_3 rocking

changes in side-group structure. It is important to note from *Figure 5* that, in going from monomer to polymer, no new infra-red bands are seen to appear. On the other hand, the relative intensities of many of the bands have changed. This is especially true of the aromatic stretching modes at ~ 1600 and 1576 cm^{-1} and of the aromatic carbon–oxygen and aliphatic carbon–oxygen stretch at 1237 and 1017 cm^{-1}, respectively. In all spectra, a strong carbon–nitrogen stretch at 1626 cm^{-1} indicates the imine functionality to be intact. Changes from the sharp well defined spectrum of the monomer (curve A) to the more rounded spectrum seen in curve C in *Figure 5* reflect the crystal–amorphous phase change that has accompanied polymerization. This phase transformation may be responsible for the changes in intensity ratios noted above. Elemental analysis results also support our belief that little if any degradation accompanies polymerization when conducted at temperatures below 200°C. Samples polymerized at 200 and 150°C show differences between theoretical and experimental mole ratios of C, H, N and O of less than 0.5%.

Earlier described d.s.c. results indicate reduced thermally induced polymerizability with increasing n in the nOBOA series. *Figure 6* shows the evolution of the room-temperature X-ray scattering profiles for the $n=1$ monomer during polymerization at 190°C. At this temperature, the monomer forms an isotropic melt. Over the course of the polymerization, there is a steady decrease in all reflections characteristic of the monomer. After approximately 30 min, an amorphous glass nearly free of crystallographic reflections remains. Visual inspection shows the sample to be transparent and dark red in colour. It is also found to be insoluble in common organic solvents. Fresh monomer forms extremely thin, sabre-like crystals that preferentially lie flat during sample preparation. From elevated-temperature X-ray scattering experiments, which show that 1OBOA forms a smectic G or H LC structure[13], the reflection at $2\theta=2.44°$ (36.1 Å) is known to correspond to the interlayer spacing in the crystal. The enhanced intensity of this peak in comparison to reflections at higher angles consequently indicates that monomer molecules are stacked along the major axis of the sabre forming 36.1 Å layers throughout the thickness of the sabre. Microscopic observation of single crystals under dark field and using a quarter-wave plate also shows the presence of discrete steps across the crystal thickness and along their edges. Such anisotropically packed samples may not fulfil the Bragg conditions needed to observe reflections that correspond to distances along the polymer chain.

Figure 7 shows a similar set of X-ray scattering profiles for fresh 3OBOA and after 30 min at 190°C. As is the case with 1OBOA, at 190°C 3OBOA is also an isotropic monomer melt. Contrary to 1OBOA however, strong and discrete reflections remain when cooled to room temperature. It is believed that the shift in the SRM reflections at wide angles and the halo at $2\theta \simeq 2°$ is probably due to a settling or positional shift of the SRM upon melting and resolidification. Whereas 1OBOA after 30 min of heating was a dark-red transparent glass, 3OBOA is still only a light-orange polycrystalline mass.

CONCLUSIONS

The above results exemplify some very interesting and new behavioural trends for semiflexible and rod-like diacetylene monomers. In the case of 1OBOA, the single methylene unit bridging the mesogenic side-group to the diacetylene core does not impart sufficient flexibility to disrupt effectively the overall rigidity of the molecule. Consequently, the imine–diacetylene–imine molecular segment behaves as a single rod-like unit. Evidence in support of this comes from elevated-temperature small-angle X-ray scattering (SAXS) experiments in which a weak and diffuse small-angle reflection was

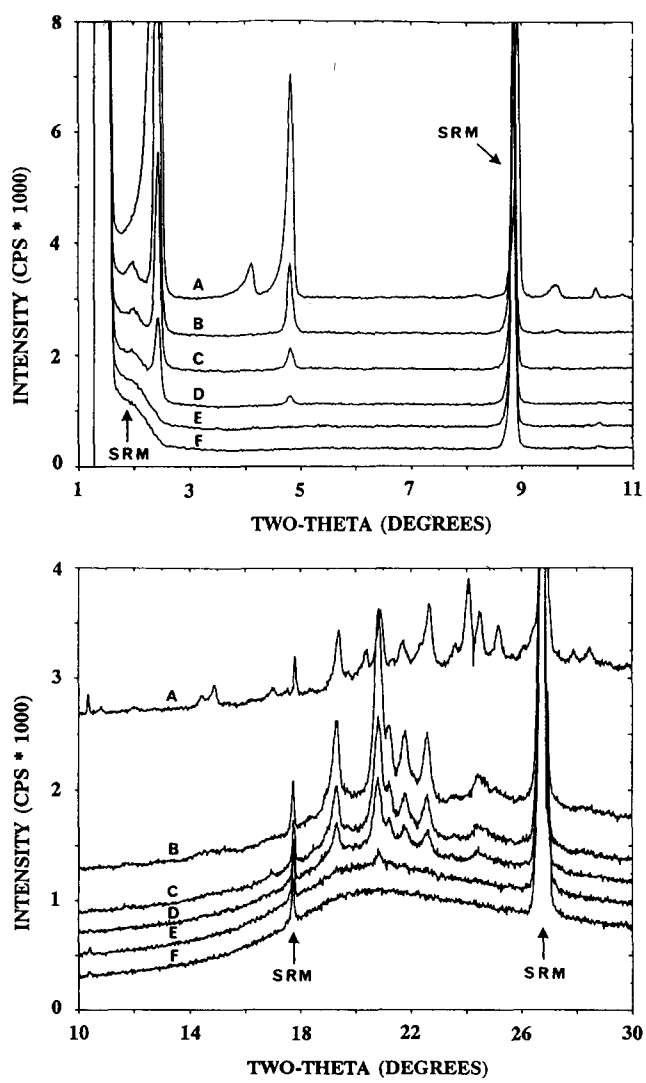

Figure 6 Evolution of room-temperature X-ray scattering patterns for 190°C 1OBOA polymerization: (A) monomer; (B) 5 min; (C) 10 min; (D) 15 min; (E) 30 min; and (F) 45 min polymerization time

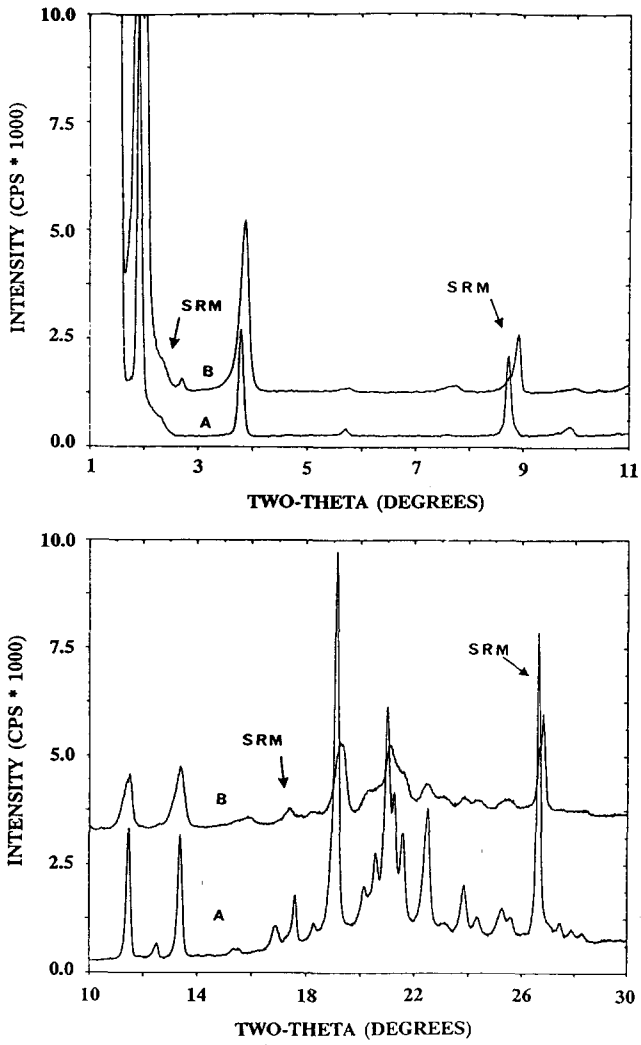

Figure 7 Room-temperature X-ray scattering patterns for 3OBOA: (A) monomer; (B) post 190°C/30 min polymerization time

observed in the isotropic monomer melt. Because of the competing polymerization pathway, with time this peak was found to disappear. Such weak scattering has been suggested to arise from intramolecular electron density fluctuations common in rod-like molecules[20]. Also, this compound exhibits liquid crystallinity over a very broad temperature range, some 50°C, suggesting that relatively few molecular configurations are accessible. In the $n=4$ case, decoupling between the imine side-chains and the diacetylene core results in an alternating flexible–rigid–flexible–etc. architecture. Consequently, simple crystal–isotropic melting is observed. In contrast to the $n=1$ homologue, high-temperature SAXS experiments of $n=4$ do not show any weak reflections when heated above its melting temperature. The molecular rigidity of the $n=3$ homologue rests somewhere in between as demonstrated by the appearance of liquid crystallinity on heating. Its persistence over only a 10°C temperature span before becoming isotropic reflects the relative instability of the regime.

Decoupling the motion of substituents from that of the diacetylene core has been examined in great detail in the symmetrically disubstituted butoxycarbonylmethylurethane (*n*BCMU) series of polymers first reported by Patel and coworkers[21]. Unlike most other diacetylene monomers, which contain a single methylene carbon bridging unit and give insoluble polymer, the $n=3$ and 4 BCMU polymers are readily soluble in common organic solvents. Similarly, whereas TS polymer is insoluble[18], poly(TS-12)[22] also gives soluble polymer. By incorporating a short polymethylene spacer into the monomer architecture, solvation of the side-grous in the polymer presumably allows disruption of the hydrocarbon backbone lattice.

The phenomenon of melt-phase polymerization of rod-like diacetylene monomers has also been seen by others. Garito and coworkers[23] have reported the synthesis and polymerization of a fully conjugated α,ω-disubstituted divinyldiacetylene (DVDA) in which nematic phase behaviour was observed on heating. As in the case of the $n=1$ homologue herein described, DVDA exhibits spontaneous polymerization within the LC region and is seen by d.s.c. to have a maximum rate at ~220°C and a heat of reaction of 210–250 kJ mol^{-1}. More recently, there have been the works of Milburn *et al.*[16,17] involving α,ω-disubstituted diphenyldiacetylenes. Though liquid crystallinity is not observed in all compounds described, spontaneous melt-phase polymerization was reported with some of the described compounds at temperatures in excess of 250°C. In addition, the melt-phase cross-polymerization of diacetylene segmented polyesters[10], polyurethanes[8] and polyamides[9] give highly coloured, elastomeric materials.

In each of the examples just described, molecular motions in the vicinity of the diacetylene linkage are either prohibited or limited due to monomer molecular architecture. In the DVDA and diphenyldiacetylene low-molecular-weight monomers, only extended molecular configurations are allowed. In the segmented diacetylene polymers, both chemical structure and the macromolecular nature of the reactant reduces the likelihood of steric overlap of the diacetylene residue by nearest neighbours. Added to this picture are the strong polymerization behavioural differences in the *n*OBOA series presented in this paper. The thermal reactivity of the three compounds studied clearly demonstrates the unique ability of rigid, rod-like monomers to polymerize in a completely disordered matrix.

Until recently, nearly all other reactive diacetylene monomers have been molecularly flexible molecules. Consequently, upon heating, not only do these materials lose all intermolecular correlations at the melting temperature, they also assume the many conformations and configurations that are thermodynamically allowed. Facile collisions between activated diacetylene residues necessary for efficient polymerization are therefore sterically unfavoured. Though 3OBOA still exhibits LC behaviour, its propensity to undergo LC or melt polymerization is severely diminished in comparison to the $n=1$ homologue. This observation for two such similar compounds indicates that monomer microstructure does not significantly affect monomer reactivity in partially disordered lattices. It would therefore seem that the function of the crystal lattice in a solid-state diacetylene polymerization is two-fold. First, it prevents the activated butadiyne unit from becoming obscured by segments of the same molecule. Second, it juxtaposes neighbouring residues within close enough proximity (0.4 nm) for polymerization to occur. The observed liquid-crystalline polymerizability of 1OBOA is consequently most likely a reflection of the inherent rod-like behaviour of the molecule rather than the particular liquid-crystalline microstructure that it exhibits.

An as yet unresolved and important question pertaining to the melt-phase polymerization of diacetylene rods is the universally observed excess heats of polymerization in comparison to conventional crystal-phase polymerization reactions. It is hoped that further examination of the linear optical properties in conjunction with nuclear magnetic resonance, resonance Raman and electron spin resonance data will shed more light on polymer backbone structure. However, it is clear from this work that rod-like diacetylene monomers can be used to prepare completely amorphous, temperature-stable films. An interesting aspect of PDAs is the high density of side-groups present within the polymer. Specifically, the substituents represent the major fraction of the overall polymer mass. Consequently, these materials offer the possibility of preparing functionalized PDAs in which now the performance of the side-group becomes the point of focus.

REFERENCES

1 Wegner, G. *Makromol. Chem.* 1971, **145**, 85; 1972, **154**, 35
2 Sauteret, C., Hermann, J. P., Frey, R., Pradere, F., Ducing, J., Baughman, R. H. and Chance, R. R. *Phys. Rev. Lett.* 1976, **36**, 956
3 Thakur, M. and Meyler, S. *Macromolecules* 1985, **18**, 2341
4 Yee, K. C. and Chance, R. R. *J. Polym. Sci., Polym. Phys. Edn.* 1978, **16**, 431
5 Bloor, D. *Mol. Cryst. Liq. Cryst.* 1983, **93**, 183
6 Schmidt, G. J. 'Reactivity of the Photoexcited Organic Molecule', Wiley, New York, 1967, p. 227
7 Baughman, R. H. *J. Polym. Sci., Polym. Phys. Edn.* 1974, **12**, 1511
8 Rubner, M. *Macromolecules* 1986, **19**, 2114
9 Beckham, H. W. and Rubner, M. F. *Macromolecules* 1989, **22**, 2130
10 Patil, A. O., Deshpande, D. D., Talwar, S. S. and Biswas, A. B. *J. Polym. Sci., Polym. Chem. Edn.* 1981, **19**, 1155
11 Schen, M. A. *Proc. SPIE, Int. Soc. Opt. Eng.* 1987, **824**, 93
12 Schen, M. A. *Proc. SPIE, Int. Soc. Opt. Eng.* 1988, **971**, 178
13 Schen, M. A., Briber, R. and Cline, J. *Polym. Prepr.* 1990, **31**, 151
14 Ozcayir, Y., Asrar, J. and Blumstein, A. *Mol. Cryst. Liq. Cryst.* 1984, **110**, 263
15 Patel, G. N., Chance, R. R., Turi, E. A. and Khanna, Y. D. *J. Am. Chem. Soc.* 1978, **100**, 6644
16 Tsibouklis, J., Werninck, A. R., Shand, A. J. and Milburn, G. H. W. *Chemtronics* 1988, **3**, 211; *Liq. Cryst.* 1988, **3**, 1393
17 Milburn, G. H. W., Werninck, A., Tsibouklis, J., Bolton, E., Thomson, G. and Shand, A. J. *Polymer* 1989, **30**, 1004
18 Wegner, G. *Makromol. Chem.* 1971, **145**, 85
19 Baughman, R. H. *J. Chem. Phys.* 1978, **68**, 3110
20 De Vries, A. in 'Liquid Crystals', Vol. 3, Proc. 3rd Int. Liq. Cryst. Conf. (Eds. G. M. Brown and M. M. Labes), Gordon and Breach, London, 1970, p. 457
21 Patel, G. N. *Polym. Prepr.* 1978, **19**, 154
22 Wenz, G. and Wegner, G. *Makromol. Chem., Rapid Commun.* 1982, **3**, 231
23 Desai, K. N., McGhie, A. R., Panackal, A. A. and Garito, A. F. *Mol. Cryst. Liq. Cryst. Lett.* 1985, **1**, 83